Calhoun

Institutional Archive of the Naval Postgraduate School

Theses and Dissertations   1. Thesis and Dissertation Collection, all items

1971

Investigation of theta-pinch produced shock waves in a plasma

Christensen, Charles Leslie

http://hdl.handle.net/10945/15784

INVESTIGATION OF THETA-PINCH PRODUCED
SHOCK WAVES IN A PLASMA

Charles Leslie Christensen

United States
Naval Postgraduate School

THESIS

INVESTIGATION OF THETA-PINCH PRODUCED

SHOCK WAVES IN A PLASMA

by

Charles Leslie Christensen

Thesis Advisor: A.W. Cooper

June 1971

Investigation of Theta-pinch Produced

Shock Waves in a Plasma

by

Charles Leslie Christensen
Lieutenant, United States Navy
B.S.E.E., Marquette University, 1963

Submitted in partial fulfillment of the
requirements for the degree of

MASTER OF SCIENCE IN PHYSICS

from the

NAVAL POSTGRADUATE SCHOOL
June 1971

ABSTRACT

This report discusses the completion and operational testing
of the theta pinch experiment at the Naval Postgraduate School
Plasma Facility. The system consists of a 42 μF capacitor bank
feeding a single turn theta pinch coil with a total energy capa-
city of 13.1 kJ. Included is a brief discussion of the theory of
shock wave generation and propagation in a plasma along with ex-
perimental verification of reproducible hydrodynamic shock waves
of Mach ~ 16 produced in a neutral Argon gas at 0.1 torr. Cal-
culations based on the theory of shock wave thicknesses (3 cm.)
are compared to observed values (10 cm.) at this pressure. An
outline of proposed future experiments at the Plasma Facility is
included in the recommendations.

TABLE OF CONTENTS

3

LIST OF ILLUSTRATIONS

ACKNOWLEDGMENT

During the completion of this project many people gave freely of their time and effort to ensure its success. Among these the following are specifically notable. To Professor A.W. Cooper who provided the impetus to see the problems encountered through to solution and who always presented an alternative approach when the going got too tough in one direction, to Hal Herreman who acted as a man Friday during the laboratory testing and development of the Theta pinch system, and the accompanying monitor circuitry, and to Mike O'Day and Bob Moeller for their expertise in design and construction of the hardware required for this project, I extend my sincere and heartfelt thanks.

To my wife Joan, who spent the last two years graciously and cheerfully in the role of a student's wife I extend my love.

Final thanks are extended to the Naval Ordnance Laboratory, White Oak, under order number P.O. 7-0034 and the Office of Naval Research which jointly sponsored this project and provided the necessary funding.

I. INTRODUCTION

This research report is a continuation of a design project initiated to study the generation and propagation of a shock wave in a plasma, with an ultimate goal of producing a collisionless shock front in a fully ionized nitrogen plasma using a Theta Pinch coil to provide the initial impulse.

Interest in this area is stimulated by the Controlled Thermonuclear Reaction (CTR) study in which confinement and heating of a plasma is a necessary prelude to the fusion reaction and by the interaction of the solar wind with the magnetosphere, the interface of which is known to be a standing collisionless shock front. Of primary interest is the energy transfer mechanism associated with a collisionless shock where the usual collisional effects between particles associated with the viscous type shocks are not encountered. The study of the plasma state in general is of considerable importance due to the effect of the ionosphere on terrestrial communications and the corresponding interruptions in these due to solar activity.

It is with the foregoing phenomena in mind that this project is undertaken in an attempt to reproduce in the laboratory under controlled conditions some of the physical situations that are observed and for which adequate models have not yet been devised.

In this report the completion and operational testing of a 13.1 kJ capacitor bank using a single turn Theta pinch coil to produce the required perturbation of the plasma is discussed along

with a brief description of the current theories regarding shock waves in a plasma. Photomultiplier observations of hydrodynamic shock fronts produced by the discharge of the bank are included with numerical evaluations of shock front thickness and velocity. The Rankine-Hugoniot equations with the effect of an external magnetic field are included for completeness along with the solutions to these equations for the special cases of propagation of the shock front both parallel and perpendicular to this magnetic field. The relations of temperature T, particle velocity u, density ρ and pressure P ahead of and behind the shock front are also included as a function of γ and Mach number for an ideal gas.

II. BACKGROUND

A. HISTORY

There have been two previous attempts at the production of shock waves at the Plasma Facility. Andrews'[1] efforts centered about the use of a multiturn coil positioned axially around the plasma column as an antenna load for an RF transmitter operating in the 100-500 kHz continuous wave mode. This transmitter was rated at 2 kW (2kJ/sec) maximum power output. This gives an energy input to the coil per cycle on the order of $(2 \times 10^3$ J/sec$) \cdot (\frac{1}{250 \times 10^3} \frac{sec}{cycle}) = 8 \times 10^{-3}$ J/cycle where a nominal frequency of 250 kHz is is used as the observed resonance frequency of the plasma column. During the course of Andrews' investigation, observation of shock wave formation was hampered by the presence of plasma column fluctuations whose source was then unknown. Further study of shock waves was abandoned by him pending localization of the plasma fluctuation sources.

In a more recent study of shock wave generation conducted by Beam [2], the RF transmitter and multiturn coil of Andrews was replaced with a .75 μF capacitor bank charged to 20 kV and a single turn pinch coil. This arrangement provided an energy input to the system during discharge of the bank of 150 Joules. Beam indicates that system results were erratic and inconsistent but photomultiplier detection of possible shock fronts yielded a signal about 2.5 times the noise level of the plasma.

It was thus determined that the underlying failure of the above
two systems to produce strong shock waves in the column could be
attributed to a lack of sufficient perturbation of the plasma. This
provided the stimulus to design and construct the current system,
initiated by Budzik [3] and ultimately completed through the op-
erational testing phase by this current study. Maximum energy
available in the system is 13.1 kJ provided by a 42 μF capacitor
bank charged to 25 kV. Reproducible shock waves in a neutral Argon
gas with Mach numbers in the range of 12-16 at a pressure of 0.1
torr (100 μ) have been achieved with the present system.

B. THETA PINCH MECHANISM

The basic principle involved in a Theta Pinch device involves
the passage of a large magnitude, short duration current pulse
through a single turn cylindrical coil surrounding a plasma con-
tained along the axis of the coil. This current causes a rapidly
increasing induction field to be propagated radially inward toward
the plasma. For a high conductivity plasma, the response is to
generate an opposing sheath current around the cylindrical circum-
ference of the plasma column in an attempt to exclude this induc-
tion field, thus leading to a $\vec{J} \times \vec{B}$ force directed radially inward
which tends to collapse or "pinch" the plasma section to a smaller
radius. Consequently, if the initial onset of the induction field
$\vec{B}_\Theta$ is rapid and the conductivity high, implying a highly diamag-
netic plasma, it is possible to generate a shock wave propagating

inward toward the coil center which carries with it the plasma
particles contained within the dimensions of pinch coil. This
description is known as the "snow plow" model of the theta pinch.

C. VISCOUS SHOCKS

This inward directed magnetic pressure wave tends to create at
the center of the coil a high particle concentration and hence a
high pressure region. Since the ends of the coil represent rela-
tively low pressure regions, this high pressure center can be re-
lieved by the formation of a pressure pulse which is vented at the
coil ends thereby. allowing for the production of a shock front which
propagates along the plasma column axis. This is the mechanism for
formation of a viscous shock front in the plasma.

During the formation of the viscous shock, if a longitudinal
$\vec{B}_o$ field exists for the long term containment of the plasma, it is
expected that the effect of the Theta pinch induction field may set
up a transverse perturbation or "kink" in this $\vec{B}_o$ field which will
propagate at or above the Alfven speed in much the same manner as
the waves on a "plucked string" where the magnitude of the $\vec{B}_o$ field
corresponds to the tension and the linear mass corresponds to the
mass of the charged plasma particles (specifically the ions)
associated with the gyromagnetic orbits along the $\vec{B}_o$ field.

D. COLLISIONLESS SHOCKS

A plasma of low density, where the mean free path for col-
lisions is large, is frequently referred to as a collisionless
plasma, an example being the aforementioned solar wind. It is

11

known that discontinuities occur in this plasma with respect to temperature, pressure and density, in much the same fashion as in a viscous shock wave. However, the dimensions of the discontinuities are much less than the collisional mean free path of the particles and such discontinuities are termed collisionless shock waves. The interface of the solar wind with the magnetosphere is such a region of discontinuities and is a good example of a collisionless shock wave.

The mechanism for this shock front is not well understood but one theory suggested by Sagdeev [4] is that a magnetic field may be formed in some manner parallel to the shock front which tends to trap the plasma particles in a gyro orbit so that the dimension of the front is on the order of a gyro radius. Such a mechanism relies on a switch on/ switch off mechanism for a shock produced induction field as described by Boyd and Sanderson [5] Chapter 6. It is noted there that the shock wave acts to refract the existing fields and in general the component of the field parallel (tangential) to the shock front is not conserved implying the shock wave contains current sheets. Verification of this shock-produced magnetic field is currently under investigation at the Postgraduate School by Davis and Case.

E. PLASMA FACILITY SPECIFICATIONS

It is instructive at this point to indicate the more common parameters of the Plasma Facility at the Naval Postgraduate School.

A more complete description may be found in Budzik [3] but the
more pertinent information is listed here for ready reference.

The plasma column is contained in a 10 foot horizontal pyrex
tube essentially composed of a 1 foot cathode-anode section and a
9 foot drift tube section. Plasma production is accomplished
through a DC discharge between the hollow cathode, which also pro-
vides the gas inlet, and a pierced disc anode, through which the
plasma penetrates into the long drift tube section and is contained
radially by a solenoidal magnetic field provided by 6 toroidal
coils positioned axially along the drift tube. At the extreme end
of the column opposite the cathode end is a floating anode which
assumes the potential of the plasma column. This is termed the
reflex arc mode of operation and essentially serves to isolate the
plasma column from the plasma source, as opposed to the glow dis-
charge type tube where the plasma column is strongly dependent on
the electric fields used to produce the discharge.

The Theta pinch experiment consists of a bank of six 7 μfd
capacitors in parallel which are simultaneously discharged through
six individual spark gaps and conducting strip lines through a
single turn, 2 in. diameter coil surrounding a section of the plasma
column.

1. Plasma Column Parameters

Confinement Induction Field $\vec{B}_o$ up to 10 kgauss homo-
geneous to within 2.5%
along axis at column

Steady State Plasma Density 10^{12}- 10^{13} particles/cm^3
for N_2 or A at 10^{-4} Torr.

Steady State Temperature
electrons   3.8-8 eV(45000-90000°K)
ions (max) $\leq$.5 eV (5000°K)

Typical collision times, calculated from Rose and Clark [6] for the following values in a typical nitrogen plasma are:

T_e Electron Temp. $50\ 000^\circ$K

T_i Ion Temp. $5\ 000^\circ$K

          Electron Density/ion density $n_e = n_i = 10^{12} cm^{-3}$

τ_{ee} Electron-Electron ~ .185 μsec

τ_{ii} Ion-Ion   ~ .98 μsec   (90° scattering of electrons by ions)

τ_{ei} Electron-ion   ~ .07 μsec

τ_{ie} Ion-Electron   ~2.8   μsec   (90° scattering of ions by electrons)

2. Theta Pinch Parameters

capacitor bank   7μ fd cap. in parallel
total inductance (calculated)   64 nh
ringing frequency   100 mHz (measured)
max charging voltage   25 kV
max stored energy   13.1 kJ.

14

III. THEORY

The theory behind shock wave formation in a plasma is still a
fertile area of research. While formation of a shock wave in a
neutral gas has been well described in the literature (see for
example, Liepman and Rosko [7] and Zel'dovich [8], this is not the
case for a plasma where coulomb and magnetic effects complicate
the processes involved. The following discussion is taken pri-
marily from Boyd and Sanderson [5] and Zel'dovich [8], and refer-
ence to these sources is highly encouraged.

A. FORMATION AND PROPAGATION OF THE VISCOUS SHOCK

Consider an initially neutral, monatomic gas, contained within
the plasma column. Passage of a large current through the pinch
coil by discharging the capacitor bank sets up large, time dependent,
electric and magnetic fields which act to ionize the contained gas.
This provides a source of free electrons and ions which, through
collisions, leads to an avalanche formation of a localized plasma
in the region of the theta pinch coil. Note that it is the fact
that ionization occurs in the neutral gas that allows the pinch
field to cause a compression. If the gas remained neutral, the gas
would be unaffected by the discharge and the pinch effect would not
occur.

Once the initial plasma region is formed, the increasing mag-
netic pressure sweeps the charged particles inward radially forming
a high density, high pressure region near the coil axis. Since the

induction field due to the discharge confines the plasma radially for a short time, (compression time) this high pressure region is relieved longitudinally along the axis of the coil in the form of a sharp-fronted pressure pulse which propagates along the plasma column as a viscous shock wave.

Since this front is composed primarily of charged particles, the residual $\vec{B}_o$ field tends to concentrate the motion along the field lines and inhibit diffusion across the field lines. Hence the $\vec{B}_o$ field acts as a channel to duct the shock front along the plasma column. Tests made both with and without this $\vec{B}_o$ field confirm this ducting action and may be noted in Figure 7.

Once the shock front has been formed, the coulomb forces act to prevent charge separation of the electrons and ions so that in general the mechanics of front interaction may be described in a first approximation by the hydrodynamic Rankine-Hugoniot equations. However the interaction of the front with $\vec{B}$ or $\vec{E}$ fields present may seriously modify observed effects compared to predictions made with these equations, and the Lorentz forces must be considered in most cases.

For reference purposes, the general Rankine-Hugoniot equations as described by Boyd and Sanderson [5] are included here with the external induction field contribution included. Note if $\vec{B}_o = 0$ these reduce to the standard Rankine-Hugoniot Equations.

B. RANKINE HUGONIOT EQUATIONS

Equation 1.

$$\left[\rho \vec{U} \cdot \hat{n} \right]_1^2 = 0$$

Equation 2.

$$\left[\rho \vec{U}(\vec{U} \cdot \hat{n}) + \left(P + \frac{B^2}{8\pi} \right) \hat{n} - (\vec{B} \cdot \hat{n}) \left(\frac{\vec{B}}{4\pi} \right) \right]_1^2 = 0$$

Equation 3.

$$\left[\vec{U} \cdot \hat{n} \left\{ \left(\rho I + \tfrac{1}{2} \rho U^2 + \frac{B^2}{8\pi} \right) + P + \frac{B^2}{8\pi} \right\} - (\vec{B} \cdot \hat{n})(\vec{B} \cdot \vec{U})/4\pi \right]_1^2 = 0$$

and $\left[\vec{B} \cdot \hat{n} \right]_1^2 = 0,$ $\left[\hat{n} \times (\vec{U} \times \vec{B}) \right]_1^2 = 0$

when the notation $[\alpha]_1^2 = \alpha_2 - \alpha_1$ is used. In these equations I is
the internal energy given by $P/(\gamma-1)\rho$ for an ideal gas, $\hat{n}$ is the
direction of propagation of the shock front, and the subscripts
1, 2 refer to the unshocked and shocked regions respectively.

C. LONGITUDINAL SHOCKS $\hat{n} \parallel \vec{B}$

For the special case where $\vec{B}_1 = \vec{B}_2$ which represents the steady state condition at the plasma facility, implying the discharge does not distort the residual field, these equations can be reduced to the standard Rankine-Hugoniot equations where the following relations hold and the numerical relations at right apply to an ideal monatomic gas.

$$T_2/T_1 \approx \frac{2\gamma(\gamma-1)}{(\gamma+1)^2} M^2 = \frac{5}{16} M^2$$

$$u_1/u_2 = \rho_2/\rho_1 \sim \frac{\gamma+1}{\gamma-1} = 4$$

$$\frac{\gamma P_2}{\gamma+1} = \frac{1}{2}\rho_1 u_1^2 \;,\; P_2 = \frac{4}{5}\rho_1 u_1^2$$

where

$$u_1 = M\, C_{S1}$$

C_{S1} = sonic speed in unshocked gas

D. CROSSFIELD SHOCKS $\hat{n} \perp \vec{B}$

For the case in which propagation of the shock front is across the field lines as in the theta pinch coil proper, Equations 1 through 3 may be solved with the result that propagation is found to be possible only at shock speeds greater than $(V_A^2 + C_S^2)^{\frac{1}{2}}$ where V_A is the Alfven velocity given by

$$V_A = \frac{B}{\sqrt{\mu(\rho_i+\rho_e)}} \approx \frac{B}{\sqrt{\mu_0 \rho_i}} = \frac{B}{\sqrt{\mu_0 n_e m_i}}$$

18

c_S is the sonic speed in the unshocked gas, and ρ_i is the ion mass density which may be written as $\rho_i = n_i m_i$ where n_i is the ion particle density (ions/cm^3) and m_i represents the ion mass.

For a neutral gas, V_A is indeterminate since $n_i = n_e = 0$, and is taken to be the speed of light, 3×10^8 m/sec, normally associated with electromagnetic wave propagation. As the avalanche phase develops, n_i increases rapidly and at 0.1 torr (100 μ) where $n_i \sim 10^{15}$ cm^{-3} for 100% ionization of a neutral Argon gas, $V_A \sim 5$-50 km/sec for a B_o field of 2 kG and it is observed that hydrodynamic shock fronts can be readily produced at the plasma facility. In the pressure range required to sustain a fully ionized steady state plasma, $\sim 10^{-4}$ torr, $V_A \sim 400$ km/sec for the same magnetic field, which implies that much higher energy inputs are required to produce shock fronts at these velocities. This is due to the inherent resistance to motion of charged particles across a magnetic field. From this it may be concluded that hydrodynamic shock fronts in the plasma regime of pressure are more difficult to produce, and no positive confirmation of hydrodynamic shock fronts in a fully ionized plasma (10^{-4} torr) has yet been verified at the plasma facility.
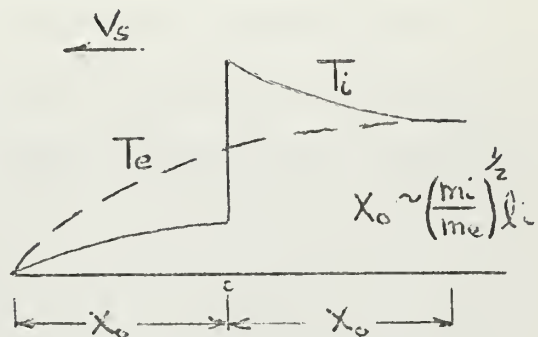
E.   ENERGETICS AND PRECURSOR EFFECTS

It is instructive at this point to consider the mechanisms of energy deposition associated with the shock wave. Zel'dovich [8] contains excellent descriptions of the processes described below and is recommended for greater detail. In general most of the

energy associated with the shock front shows up in kinetic

energy of the gas particles and hence in a temperature increase in

the shocked gas coupled with a pressure and density increase.

There are other mechanisms active however and a brief description

of these follows.

1. Electron Heat Conduction

It was initially noted that a number of "priming" elec-

trons were produced during the discharge and avalanche formation

of the plasma and shock front. These initial high speed electrons

receive their energy from the high electric fields generated and

hence some of the energy associated with the shock is tied up in

these high speed electrons. In a normal elastic collision pro-

cess a maximum fraction of the energy $\dfrac{4m_a m_b}{(m_a + m_b)^2}$ may be trans-

ferred to the second particle in the collision. If this particle

is an electron, a rapid transmission of this temperature can be

spread through the gas by means of electron heat conduction and

this process is active in shock front passage. The heated elec-

trons rapidly transmit their temperature through the shock front

and in effect preheat the gas ahead of the shock front. A profile

of this electron preheat region, described by Zel'dovich [8] Vol.

II Ch 7 is shown in the accompanying diagram. Also shown is the

ion temperature profile. The ions, being much more massive than

the electrons have their kinetic energy increased by passage of

the shock front, but since their velocity is of the same order as

the shock speed, no preheating ahead of the shock front is attri-

buted to the ions. The increased ion temperature ahead of the

shock is due to the equilibration tendency of the precursor

electron temperature profile T_e. Eventually the ions and electrons

attain thermal equilibrium
at some later time after shock
passage. Relating the luminosity
of the gas to the temperature,
the profiles shown in the accom-
panying figure can be used to
describe qualitatively the effects
of the shock front passage and
lead to an analysis of the preheat

Ion and electron (dashed)
temperature profile of a
shock front in a cold plasma.
Zel'dovich [8] Ch 7.

region ahead of the shock. An excellent theoretical description

and computer solution to this problem is presented by Shafranov [9].

2. Excited States

For a monatomic gas, there are no molecular vibrational

or rotational levels and any energy increase in the gas shows up

as ionization or excited atomic levels. Thus most of the energy

input to the system shows up as energy of the shock front which

can be characterized by a Mach number. In the case of a diatomic

gas, some of the input energy may be absorbed internally by the

gas to excite molecular rotational or vibrational levels with the

consequence that less of the initial energy is available as energy

of the shock front per se. This represents a weaker, less ener-

getic front, i.e., a lower Mach number, with the result that the

difference in gas parameters across the front; T, ρ, and P will

not be as great as for the monatomic case. In other words,

production of similar strength shock waves require higher energy
inputs in the case of diatomic gases. This point was illustrated
in this investigation for the case of Argon and Nitrogen gases
where it was noted that shocks are readily generated in Argon but
are very difficult to achieve in Nitrogen with the same voltage on
the capacitor bank.

3. Radiation from the Shocked Gas

Photons emitted from the excited ionized region behind
the front are emitted isotropically in all directions. Some of
these penetrate the shock front and are absorbed in the unshocked
region which results in a preconditioning of the unshocked gas and
retention of energy in the system. However, those photons which
are not absorbed in the gas ahead of the shock front essentially
escape from the system, which has the effect of removing energy
from the gas by radiation and causes a dispersion of the shock
front due to this energy loss. This radiation results in a cooling
of the gas behind the shock front with a corresponding density in-
crease. Hence, radiation from the gas represents an energy loss
mechanism and provides a method of dispersion of the shock front
energy. In this vein, while the effects of radiation flux re-
presents an energy loss, the effect of radiation pressure is
usually negligible compared to the collisional gas pressure.
Zel'dovich [8] notes that the radiation pressure becomes comparable
to the hydrodynamic pressure only at $T \sim 3 \times 10^6 K$ in atmospheric
air.

4. Velocities and Thicknesses of Shock Fronts

As has been noted previously, in the case of viscous shocks, since coulomb forces prevent large degrees of charge separation, the shock front can be treated as a typical un-ionzed front for which the Rankine-Hugoniot equations apply in a first approximation. In this case the characteristic speed is the sonic speed C_S and the ratio of shock front velocity to C_S is defined as the Mach number M. This Mach number is specifically derived both by Jukes [10] and Jaffrin [11] and is quoted below.

$$M^2 = \frac{M_i U_i^2 + M_e U_e^2}{\gamma_i k T_i + \gamma_e k T_e} \approx \frac{M_i U_i^2}{2\gamma_i k T_i} \quad \text{for} \quad \begin{array}{c} T_e = T_i \\ \gamma_i = \gamma_e \end{array}$$

The shock front thickness is determined by the ion-ion collision time, and hence is on the order of an ion mean free path $\ell_i \sim V_S \tau_{ii}$ where V_S is the shock speed. During the time τ_{ii}, the ion gas cannot transfer any significant energy to the electrons due to the long $\tau_{ie} \propto \left(\frac{m_i}{m_e}\right)^{1/2} \tau_{ii}$ and since the increase in electron temperature due to electron viscous forces is small, the mechanism of electron heat conduction noted in III, E, 1 represents a more probable process.

In the case of Alfven wave propagation, which involves no mass transport, since these are transverse waves, the discussion of shock front thickness is not applicable.

In the case of collisionless shocks it has been noted in section D of this chapter that propagation is only possible at

speeds greater than $(V_A^2 + C_S^2)^{1/2}$ for crossfield shocks. A further consequence of the theory of the tangential component of $\vec{B}$ parallel to the shock front restricts the thickness of the front to the order of a Larmor radius for the charged particles. This dimension seems to be verified by the Tarantula experiment cited by Boyd and Sanderson [5]. Along this same line Shafranov [9] notes that a severe degradiation in the electron heat conduction effect occurs in cases where a magnetic field exists parallel to the shock front, presumably due to a restriction of the normal electron-electron collisions across the front. This is precisely the case for shock waves generated within the Theta pinch coil.

To account for the profile of electron heat conduction noted in 5A, Zel'dovich [8] shows that the preheat region ahead of the shock is of the same order of length as the relaxation region behind the shock and can be approximated by

$$X_o \sim \left(\frac{m_i}{m_e}\right)^{1/2} \lambda_i \propto T_i^2 \propto V_s^4$$

From this it can be seen that the higher strengh shocks are preceded by a longer preheat distance and the advance of the shock front is "telegraphed" considerably ahead into the unshocked gas.

IV. OPERATIONAL COMPLETION OF THE THETA PINCH INSTALLATION

The sections listed below represent the hardware problems encountered during the initial completion/testing phase of the Theta pinch experiment.

A. FRACTURE OF GLASS COLUMN

The system of capacitor bank circuitry and ducting of the current pulse through the strip lines to the Theta pinch coil was completed in the work by Budzik [3]. However, during discharge of the bank, the glass column within the pinch coil was fractured and diagnosis of this fault formed the starting point for this current project. Two possible causes were determined to be (a) expansion-contraction of the coil due to reaction to the current pulse and/or (b) whipping of the pinch coil due to flexing in the strip lines during discharge.

An order of magnitude calculation of the possible expansion-contraction dimensional change due to the current impulse showed that adequate clearance was maintained between the coil and the glass for all ranges of bank voltage. To confirm this, the coil was moved for better access and several firings with a section of the glass tubing installed but unsecured at the ends resulted in no fracture of the glass. Hence it was concluded that the fracture was due to the whipping of the coil.

During this stage of testing it was noted that the coil was not exactly round for the full length (6") and installation of the glass tube resulted in breakage on one occasion due to

misalignment. This was remedied by inserting a 1/16" copper shim in the conducting joint and a 1/16" plexiglass shim diametrically opposite to this joint. This allowed an extra margin of tolerance and no further glass breakage occurred.

B. CONSTRUCTION OF MICARTA COLLAR

Since the glass fracture was traced to the whipping of the coil, a Micarta Collar was designed and constructed to fit over the ends of the pinch coil which was then braced to the internal structure of the facility. This collar and bracing structure is shown in Figure 1A. This configuration is such as to hold the pinch coil rigid at the plasma column and reflects any flexing tendency back down the strip lines where it can be readily absorbed. There has been no further fracture of the glass tubing in any of the subsequent firings of the bank.

C. RESEALING OF THE SPARK GAPS

During the testing of the pinch coil noted above it was found that some of the Spark Gap boxes had developed leaks and could no longer be pressurized. Since the pressure of the Nitrogen in the boxes is the primary factor in maintaining the stand off potential of the gaps, this presented an immediate problem. It was determined that the leaks occurred at the copper-plexiglass bond where the strip lines entered the spark gaps. The original construction allowed for an epoxy seal at this point but in the curing process and under the aforementioned flexing of the strip lines, this seal had become brittle and failed.

As a stop gap measure, a 1/8" layer of a second epoxy mix, chosen for its flexible consistency when cured, was poured onto the floor of the defective spark gap containers. This resulted in a semi-soft sealant which tended to form a tighter bond under pressurization in the fashion of an "O" ring seal, thus eliminating the leak.

This modification was made to the three spark gaps which were found to be defective and is so effective that pressure can be maintained in the system in excess of 48 hours. The epoxy used was EPO cast 4-L with hardener 9112 in a 5 to 1 ratio by weight of epoxy to hardener.

The master box was noted to have a small leak but was not modified since pressurization could be maintained and since this box has a separate pressurization tank. Pressure can be maintained for 30 minutes in this box with the system secured.

D. CONSTRUCTION OF REPLACEMENT SPARK GAPS

When the leaks were detected in the spark gaps, construction was started on replacements. These boxes are ready for completion pending incorporation of the epoxy sealant between the outer shell of the box and the internal plexiglass former used to support the strip lines in the box interior. Application of the sealant in this region should insure a virtually leakproof container.

E. DESIGN AND CONSTRUCTION OF THE MONITOR SYSTEM

Completion of the above steps permitted test discharges of the capacitor bank. These first runs were done in air to monitor the magnetic probe pick-up inside the pinch coil. Testing during this

phase was inconsistant and a decision was made to monitor the individual spark gaps for proper operation. In this manner, at least a relative figure of merit could be assigned each discharge based on the energy of the bank and the number of capacitors which discharged.

The monitor circuit designed for this purpose is shown in Figure 1B. The basic operation is described herein. Light from the discharge is routed into a chamber through the sight tube and energizes the photo transistor circuit. This in turn triggers the SCR into conduction and completes the lamp circuit. In this way, each box is monitored on each run and knowing how many boxes discharged indicates the energy input to the coil. The potentiometer is incorporated to permit adjustment of the sensitivity of the trigger circuit and the .02 μF capacitor acts as an R.F. bypass around the SCR to eliminate spurious triggers.

The entire circuit is mounted on a Micarta board and installed in a conducting housing and mounted near the corresponding spark gap. The housing is grounded at the light panel to the internal circuitry of the box, but no connection between the internal cir-cuitry and the housing is made at the spark gap location. In this way a Faraday shield is provided by the housing to eliminate spu-rious triggers in the common circuit.

All parts were obtained locally and are standard off-the-shelf items. The power supply is a standard transistor power supply and total circuit current is 400 MA at 22 VDC. Operation of the

monitoring circuit has been completely successful and has provided
the additional service of localizing the offending spark gap when-
ever misfires or auto discharges of the bank occur. It also allows
a record to be maintained of each spark gap discharge for pre-
ventive maintainance applications.

F. MINOR SYSTEM MODIFICATIONS

  1. Enlargement of Stand Pipe

      Monitoring of the effects of the discharge of the bank was
expected to be through the use of magnetic probes described by
McLaughlin [12] inserted into the plasma chamber. The original
glass section used in the theta pinch coil was equipped with a
2 inch standpipe for insertion of the probe into the chamber.
This standpipe was designed to accept a probe of 5 mm outside
diameter. However, some of the probes which were constructed had
a 6 mm OD and could not be utilized. Thus it was decided to
enlarge the standpipe ID to allow acceptance of probes up to 7 mm
($\frac{1}{4}$") OD. In this way, if cooling of the probes becomes necessary
there is already built into the system additional tolerance for
larger probe diameters. It has been shown by McLaughlin that
heating of the probes in the plasma column center will be a problem
and the life expectancy in the center of the column is on the order
of 2 seconds under typical plasma operating conditions. Thus a
provision for cooling the probes is a problem of concern in the
future.

2. Enlargement of Camera Port

It is anticipated that a high speed camera may be available for application at the facility and so provision has been made in the pinch coil to allow photographs to be made of the pinch effect on the plasma during discharge of the bank. A segment 3/8" by 1" has been removed from the coil to allow visual access to the plasma column inside the coil. Thus light from the column may be ducted to the camera by means of a ribbon light pipe to allow study of the dimension changes in the plasma during discharge. These changes to the coil are represented in Figure 2.

3. Coating of Strip Line Joints

While the Theta pinch coil was accessible during the testing for glass breakage, the joints in the strip lines were treated with a conducting grease. This was deemed necessary due to the anticipated high resistance of these joints under the discharge current. Results to date attribute no difficulties in this area.

V. RESULTS IN TESTING

While this testing has in general been exploratory in nature
some quantitative results have been obtained. In the discussion
that follows the main bank charging voltage has been maintained
at 15 kV unless otherwise noted. The circuit used to charge the
main bank capacitors is equiped with an over-current circuit
breaker which trips if the charging current becomes too high. With
the present bank configuration, the system can be charged to 15 kV
without tripping this relay. However, if a charge voltage is de-
sired greater than 15 kV, the circuit must be energized first at
15 kV until the initial current surge ceases and then manually
stepped up to the desired voltage. This process is time consuming
and not conducive to precise duplication from shot to shot. Thus
for operation at voltages in excess of 15 kV, two men are required
for efficient operation, one monitoring the charge and the other
operating the oscilloscope used to record the data. Since the
initial testing was qualitative in nature, the 15 kV operating
range was adequate to establish operating procedures.

A. PRESSURE RANGE FOR SPARK GAPS

The first problem encountered once the Theta pinch coil was
rigged in position was that of determining the correct pressure in
the spark gaps to ensure a discharge during a trigger from the
master gap, but to prevent a self-initiated discharge. A system
circuit diagram is shown in Figures 3A and 3B. As in any spark

gap circuit, results are somewhat inconsistent but the Pressure

versus Voltage schedule shown in Figure 4 depicts the general

behavior of this system. Note that the region between the "no

fire" (high pressure) and "auto fire" (low pressure) becomes much

narrower with increasing voltage. Hence operation at voltages

above 20 kV is extremely pressure-sensitive. As a rule of thumb,

satisfactory operation can be achieved in the 12 kV - 18 kV range

if a pressure in PSI equal to Bank Voltage in kV schedule is

followed.

B.   REQUIREMENTS ON RISE TIME OF CURRENT PULSE

One of the motivating reasons behind the construction of the

Theta Pinch system was the desire to produce a collisionless shock

wave. From the theory it can be shown that one of the conditions

necessary to produce the desired effect is that the rise time of

the current pulse be on the order of the ion-ion collision time,

~ 1 μsec or less, and also in the range R/V_A where R represents

the radius of the coil. It was noted in III, D that propagation

across the field can only occur if the shock speed is greater than

$(V_A^2 + C_S^2)^{\frac{1}{2}}$. The Alfven speed, as noted earlier can be calculated

from

$$V_A = \frac{B}{\sqrt{\mu_0 \rho_i}} = \frac{2.19 \times 10^9 \, B \, [\text{GAUSS}]}{\sqrt{n \, [\text{IONS/CM}^3] \, m \, [\text{AMU}]}} \, \text{M/S}$$

32

At the plasma facility using an Argon gas at 10^{-4} Torr with a $\vec{B}_o$ field of 2 kG, $n_i \sim 2.5 \times 10^{12}$ ions/cm^3 yields a value of $V_A \sim 400$ km/sec. Then for R = 2.5 cm we get a travel time to the center of the column $R/V_A \sim .05$ μsec. Thus it is desirable to have the rise time of the current pulse between .05 μsec and 1 μsec.

From the discharge of the capacitor bank, an initial ringing frequency on the order of 110 kHz was determined. Thus, considering this as a sinusoidal wave, the time from 0-90% of the maximum amplitude occurs in the first $64^\circ \sim 1/6$ of the cycle. Thus the measured rise time is given by $1/6 \times (1/110$ kHz$) \sim 1.5$ μsec which is only slightly outside the range noted above. Improvements on this time require either a decrease in the capacitance of the system and hence loss of energy storage capability or a decrease in circuit inductance. This latter is a difficult task since the system was specifically designed for minimum inductance. Hence continued operation must be conducted with this restriction in mind.

C. 110 kHz, 20 kHz COIL OSCILLATIONS

From the circuit parameters contained in Budzik's Thesis [3] a predicted ringing frequency of 97 kHz was expected so this 110 kHz signal observed confirms the values of the circuit parameters. However it was noted during attempts to monitor magnetic probe pick-ups down stream from the pinch coil that a very weak signal in the range of 20 kHz could be detected. This signal is the lower trace in Figure 5B with the Theta Pinch discharge signal shown in Figure 5A. In Figure 5B the upper trace has a scale of

33

1v/cm, 10 μsec/cm while the lower trace has a scale of .5 mv/cm, 50 μsec/cm. The two traces are generated by the same probe. It can be seen that the first 50 μsec of the lower trace (5 divisions of upper trace) are completely off scale but as the upper trace signal damps to 0, (~ 70 μsec), a second signal is picked up on the lower trace with a frequency of 20 kHz. The source of this signal has not yet been determined but is presumed to be caused by secondary oscillations of some part of the facility which are triggered by the primary discharge.

This 20 kHz signal has not interfered with any of the operations of the system but its presence is noted here for completeness.

D. HYDRODYNAMIC SHOCK WAVE OBSERVATION

Initial detection of the hydrodynamic shock front was attempted using a magnetic probe located downstream from the Theta pinch coil on the assumption that currents presumed to be associated with the front would be detected by the probe. Several attempts at this method of detection yielded no meaningful results so it was decided to correlate the probe pick up signal with a photomultiplier at the same position. The experimental set-up is shown in Figure 6. It was during this phase of testing that the need for the spark gap monitors, described earlier, arose to permit correlation of the luminous front with energy input to the coil.

A representative series of photographs to indicate the effects of various experiment parameters is contained in Figure 7 and is described below. This series was taken with a neutral argon gas at 0.1 torr (100 μ) pressure with a bank voltage of 15 kV. The sonic speed in argon at this pressure is taken as 310 m/sec for the calculations. The photomultiplier was located .635 m(25") downstream of the pinch coil.

The initial rise of the light pulse occurs at a time on the order of 140 μsec in 7a. and 120 μsec in 7b. This corresponds to a shock speed of .635/$\dot{t}$ = 4.5 km/sec and 5.3 km/sec respectively with corresponding Mach numbers of 14.5 and 17. From these, the effect of the residual $\vec{B}_o$ field on the shock front is noted. At the lower value of $\vec{B}_o$, the shock speed is somewhat lower presumably due to diffusion of the shock front particles across the field. As the field strength is increased, this diffusion process is inhibited and a more energetic shock front is obtained. In 7c. with $\vec{B}_o$ = 0 and the remaining parameters held fixed, no shock front is observed, indicating that the energy pumped into the gas during the discharge is rapidly dissipated in all directions and the anisotropy caused by the $\vec{B}_o$ field is no longer present.

The effect of misfires or delayed fires in the spark gaps is shown in 7d. This represents a shock caused by the discharge of 4 of the 6 capacitors in the bank with a consequent degradation of energy input to the coil and a distortion of the current pulse

shape, presumed to be due to non-simultaneous discharge of the spark gaps. Using again the initial rise of the pulse as the start of the shock front we get a shock speed of 1.8 km/sec with a Mach on the order of 6 which represents a severe degradiation of the shock front energy.

From these and other runs the following observations and effects have been noted. Rather consistent results have been obtained in the .01 - 0.1 torr (10μ - 100μ) pressure range for a neutral Argon gas and these are summarized below.

1. $\vec{B}_o$ - acts as the confinement field for the shock tube and provides the anisotropy or ducting effect along the axis of the column. Increasing this field concentrates the discharge energy in the front and inhibits dissipation of the front due to diffusion processes.

2. Bank Voltage: This determines the energy that can be deposited in the gas column through the pinch coil. The effects of misfires or non-simultaneous discharges severely affects the associated shock strength and profile.

3. Column Pressure: This parameter has little affect on the shock strength but controls the luminous period following the front, ranging from a typical value of 300 μsec at 100μ to about 100 μsec at 10μ. This is expected to be the result of the decreased density of excited atoms at 10μ and hence a lower intensity of radiation.

E. SHOCK FRONT THICKNESS

As a frist order determination of the shock front thickness
the time between the initial rise and the first dip in the photo-
multiplier signal of Figure 7B is used as $t \sim 20$ μsec which gives
a thickness $\ell \sim (5.3$ km/sec$)(20$ μsec$) \sim 10$ cm. Zel'dovich notes in
Chapter 7 page 512 that at $P_o \sim 10$ mm Hg a shock front thickness of
$\ell_o \sim .03$ cm is obtained at $M = 16.3$ and notes these values are
inversely proportional to the gas density. Thus it is expected
that for $\ell / \ell_o \propto \rho_o / \rho$ and noting that the density is proportional
to the pressure ($P = \rho RT$),

$$\rho_o / \rho = P_o / P = \frac{10 \text{ mm}}{0.1 \text{ mm}} = 100$$

gives $\ell \sim 100 \ell_o \sim 3$ cm so the value of 10 cm noted above is in
order-of-magnitude agreement with expectation.

F. HYDRODYNAMIC SHOCKS IN PLASMA

Observation of a hydrodynamic shock front in the region of
pressure required to sustain a plasma ($\sim 10^{-4}$ Torr) has not been
verified to date at the Plasma Facility. Figure 8 shows the re-
sults of the downstream photomultiplier pick-up described in D
above with an Argon plasma at 10^{-4} Torr and $B = 1800$ Gauss. The
results show that the light pulses occur in the same time frame
as the Theta pinch discharge (50 μsec) and hence are presumed to
be due to an electromagnetic ionization wave in the plasma. No
indication of a following hydrodynamic shock front in a time up
to 500 μsec following the discharge was observed. It may be noted

that at this pressure the plasma is essentially collisionless which may account for the absence of a hydrodynamic shock front. Operation at bank voltages greater than 15 kV may produce the desired effect and forms a basis for continuing investigation.

The lower trace in the photographs represent a pick-up of the 20 kHz signal noted earlier and correlation with the photomultiplier output is not intended.

G. TRANSVERSE DISTORTION OF $\vec{B}_o$

The final area of study involved the theory of the "kink" disturbance in the residual magnetic field. Propagation of the "kink" was expected to be at the Alfven velocity. Thus for B_o = 3600 Gauss and assuming 1% ionization of the argon gas at 0.1 torr (100μ), $(\rho_i \sim 2.5 \times 10^{13}$ ions/cm$^3)$ gives $\bar{V}_A \approx 250$ km/sec. Figure 9 which relates the signals from the Theta pinch magnetic probe and the downstream (.635m) magnetic probe shows a time separation between the wave forms on the order of 2 μsec. This corresponds to a velocity of 300 km/sec. This phase separated signal may be the desired "kink" of interest in the $\vec{B}_o$ field but experimental results have been inconsistent in this area primarily due to the uncertainty in the degree of ionization. Duplication of this signal has been unsuccessful on two successive occasions and is attributed to a small leak in the vacuum chamber causing a contamination of the Argon gas with Nitrogen. Zel'dovich [8] indicates that the impurity content of Argon significantly affects the experimental values obtained.

H. OBSERVATION OF THE COLLISIONLESS SHOCK FRONT

As noted in the theory section, the possibility exists of the production of a collisionless shock front in the region of the Theta pinch coil. The passage of this front is expected to be accompanied by current sheets which may be detected with the magnetic probes. However, this method of detection requires that the probes be inserted into the plasma column and as noted earlier, the life expectancy of the probes in this configuration is about 2 seconds under typical operating conditions. Thus, if probes are to be utilized for detection, they must be cooled. To date no provision is available for cooling these probes and further investigation of this shock front must be delayed pending more sophisticated detection methods.

A possible solution is a mechanical device to drive the probes into the column just prior to discharge of the bank and withdraw them immediately thereafter. The probe need be in the column for less than 100 µsec which is the time frame for complete discharge of the bank, but such a mechanism represents a formidable engieering task due to the limited space in the coil region and the requirement to maintain the system vacuum. A more tractable solution lies in the possible cooling of the probes with either forced air or liquid air. This may be achieved by a suitable probe modification and the increased standpipe ID of the pinch coil glass mentioned in IV, F1 was implemented with this problem in mind.

VI. CONCLUSION

The Theta Pinch experiment is now completed and ready for
extensive operation. The basic system has been shown to be fully
operational in all aspects and system operating procedures es-
tablished. These are contained in appendix A of this report.
Hydrodynamic shock waves have been produced in the $M \approx 15$ range
in a neutral Argon gas at 15 kV. Further study in the plasma
range of pressure is now possible as is investigation of the
collisionless shock front regime.

VII. RECOMMENDATIONS

The recommendations given here can be divided into two parts, a System Study, and an Experimental study. These are noted briefly below.

A. SYSTEM STUDY

Inspection of the spark gaps shows signs of deterioration of the electrodes. It is recommended that one or two of these spark gaps be replaced if possible with those from the original experiment done by the Garching group cited by Budzik [3]. Many of the problems in duplication are directly attributable to the spark gaps and use of the more permanent fiberglass molded gaps noted by Budzik may alleviate these problems.

In any case the spark gaps currently under construction must be completed. In this same vein, a quantitative relation between Pressure and Voltage must be determined to permit more reproducible results in the 20-25 kV range.

B. EXPERIMENTAL STUDIES

A more detailed profile of luminosity versus time must be obtained for the time period $0 \rightarrow 500$ μsec for the neutral Argon Gas as a function of Bank voltage, $\vec{B}_o$ and Pressure, to permit more detailed study of the shock front. Correlation of T and ρ behind the front with values predicted by the Rankine-Hugoniot equations is also necessary. Similar studies for diatomic gases is a possible

extension of the above study. Spectroscopic study of the wave front will indicate the types of ionization/excitation associated with the front.

Similar effects of the above studies can be made on a plasma along with the study of the collisionless shock front predicted in the plasma regime. Cooling of the probes will be required to permit study of the plasma interior necessary for this latter project. Correlation with a high speed camera may help describe the shock profiles expected.

In the above studies correlation of magnetic probe signals with photomultiplier signals is anticipated to be the primary diagnostic technique available for these experiments. Density variations are most easily measured using microwave interfero-metric methods but this facility is not available locally. Thus laser scattering techniques, currently under investigation at the plasma facility, may become necessary.

This is but a small list of the projects that are now possible with the current Theta Pinch facility.

APPENDIX A

THETA PINCH OPERATING PROCEDURES

Pre Inspection:

1. Check that strip lines and spark gaps are clear, no foreign objects.

2. Pressurize boxes: Master 35 PSI } Nominal. See P.vs.V.
    Slave(6) 25 PSI } Curve Figure 4.

3. Remove C clamps from Cap. Bank (6).

Turn On

Master Hi V. Ckt.

1. Ckt Bkr 10. on Main Power Panel (this powers the Stanford Pwr. Sup.)

2. Control / Fan / Hi V / Rect. Fil. Ckt Bkrs On

3. Press System Start (2 min. delay)

4. Press Hi voltage Start Button

5. Rotate Hi Voltage control to desired voltage (35 kV @ 35 PSI).

Main Bank P.S.

1. 4 ckt Bkrs on lower left hand panel ON.

2. Press Hi voltage Button ON, Set Voltage to Max Desired charging voltage for main Bank. Do not exceed 25 kV. (Red Line)

3. Set microammeter on Relay cage to max desired voltage; (optional) Note that meter reads 0-20 amp → 0-25 kV max so the scale factor is (1.25) x (meter reading) = Cap. voltage.

Main Control Console:

1. Turn Power Switch (lower right hand panel) ON.

2. Set Hi V. Trigger meter to 12.5 kV.

43

3. Set Hi V current to 17-18 ma.

4. Purge both Master and Slave gaps.

5. Press Master Charge Button. Red light indicates charged.
   Press Main Bank charge button, lower Red light indicates
   charging. Upper Red light indicates charged.

6. To discharge Main Bank press Fire button.

7. Repeat steps 4-6 to refire bank.

Shut Down

Press both dump switches. Follow reverse order of turn-on
procedure.
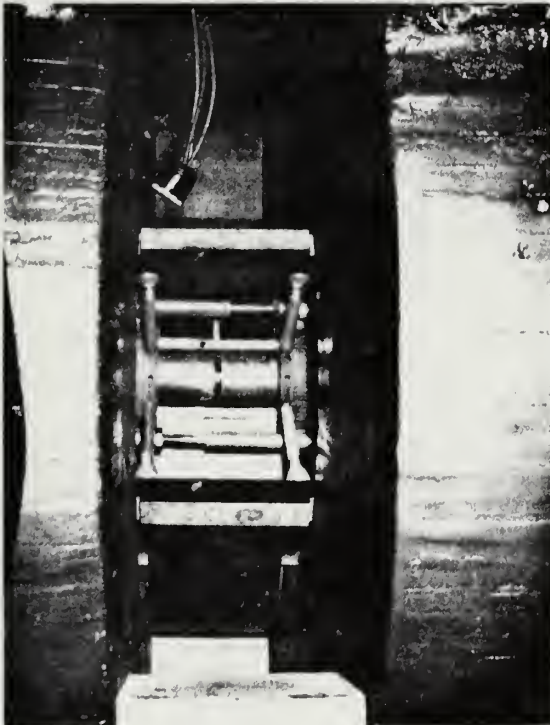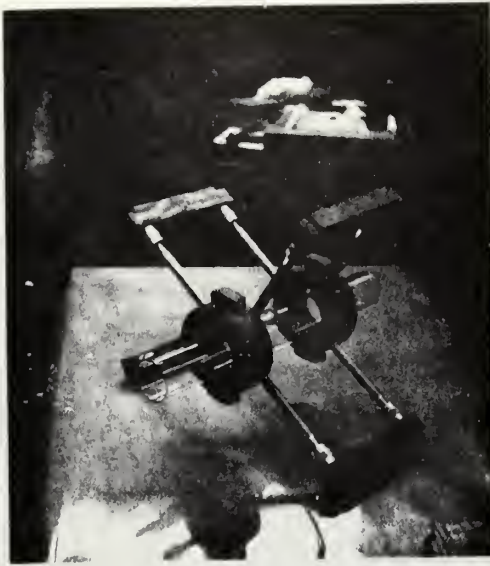
Micarta collar designed
to hold pinch coil rigid:

Above photographs show
relative location of
collar and glass column.

Left photograph of collar
installed on the pinch
column.

Figure 1A.   Photographs of Micarta Collar

MONITOR CIRCUITRY
1 OF 6 CHANNELS

SHOWN FOR SPARK GAP #1

LIGHT POST

MONITOR
HOUSING

62k

SCR

PHOTO
TRANSISTOR

5K

SENS

10K

1M

10K

6V
Z.D.

SHIELD

RED
WHITE
BLACK

.02μf
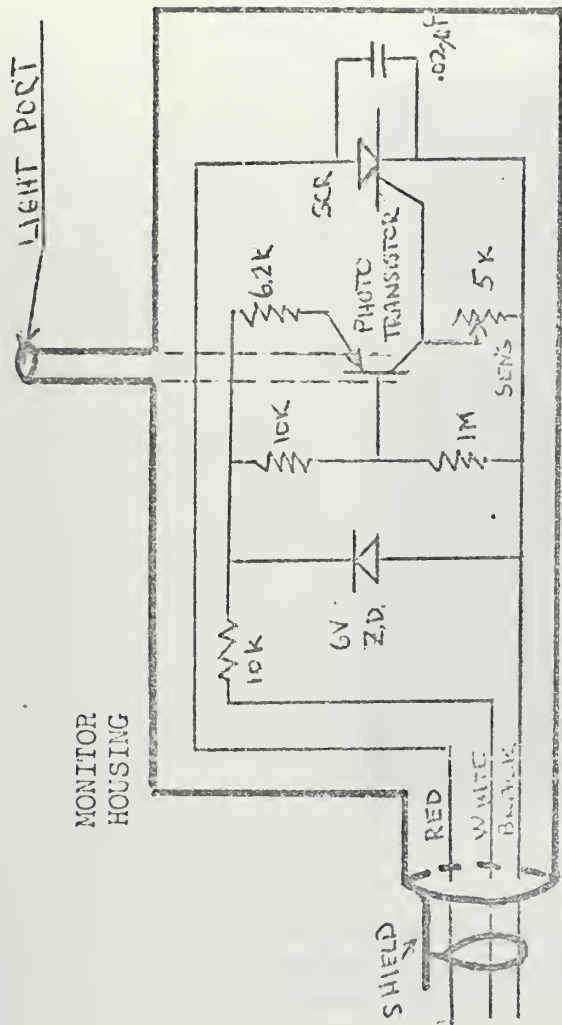
ACTIVE ELEMENTS

Z.D. ZENER DIODE 6 VOLT
PHOTO TRANSISTOR NAA 469
SILICON CONTROLLED RECTIFIER
2N 2326

TRANSISTOR POWER SUPPLY
22 VOLTS, 400 MA.

WHITE
RED
BLACK

OFF
ON

PUSH
TO
RESET

SPARK

2 3 4 5 6

+22V D.C.
TRANSISTOR
PWR
SUP

LAMP PANEL
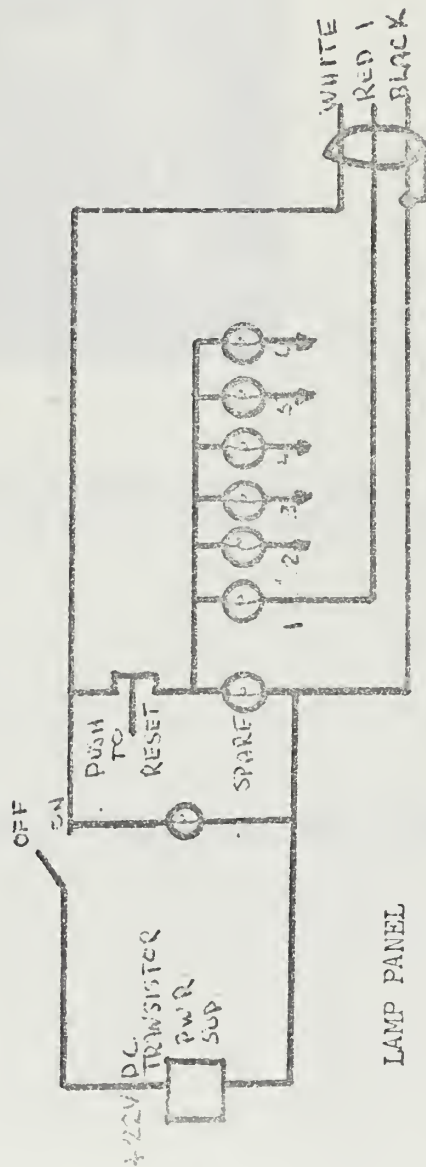
Figure 1B. Monitor System Circuitry

46

Capacitor bank assembly showing spark gaps, (a),
monitor boxes (b), and strip lines (c) to theta
pinch coil

Figure 1C.   Photograph of Capacitor Bank Assembly
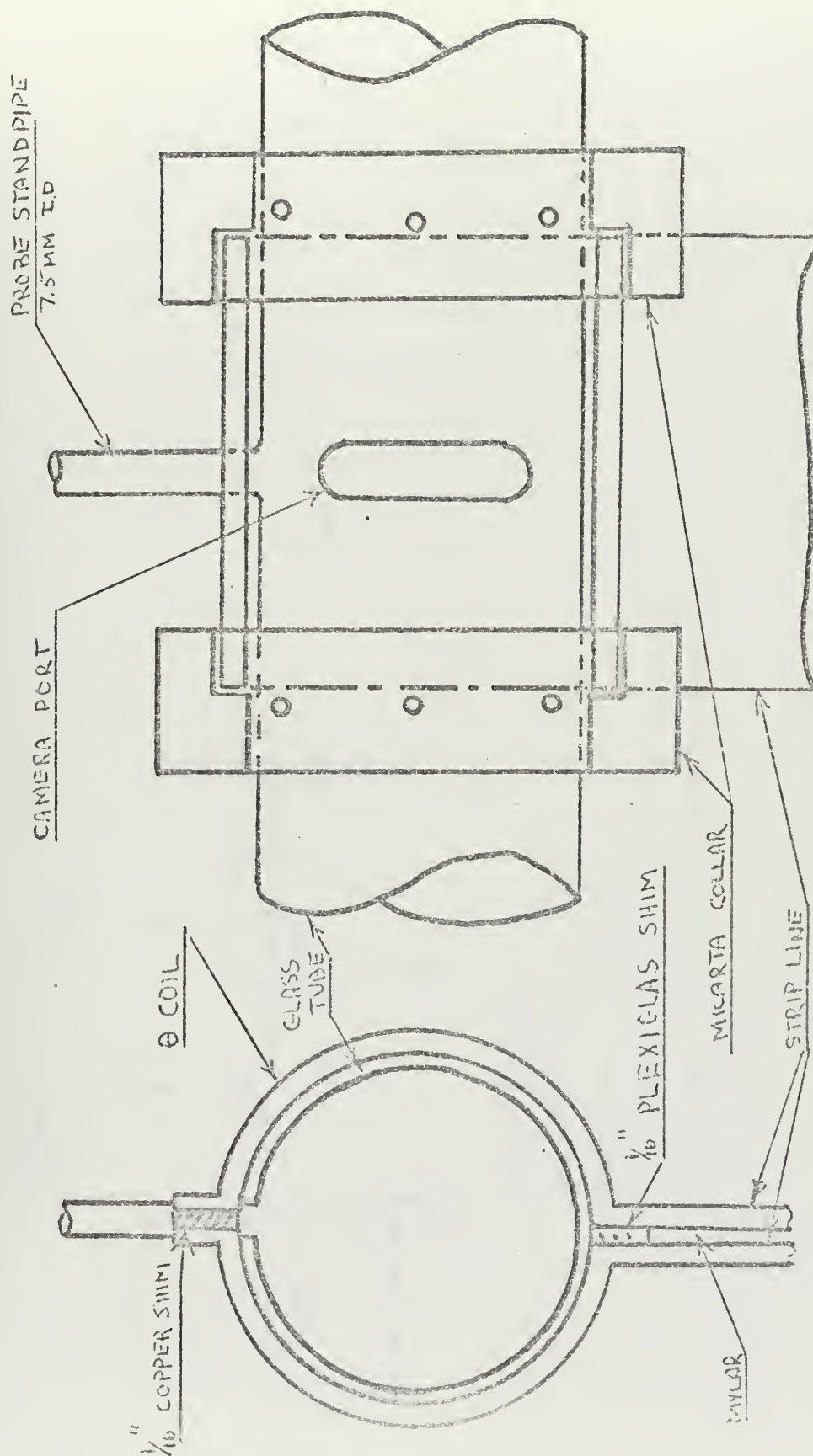
Figure 2. Modifications to Theta Pinch Coil and Glass Column

48
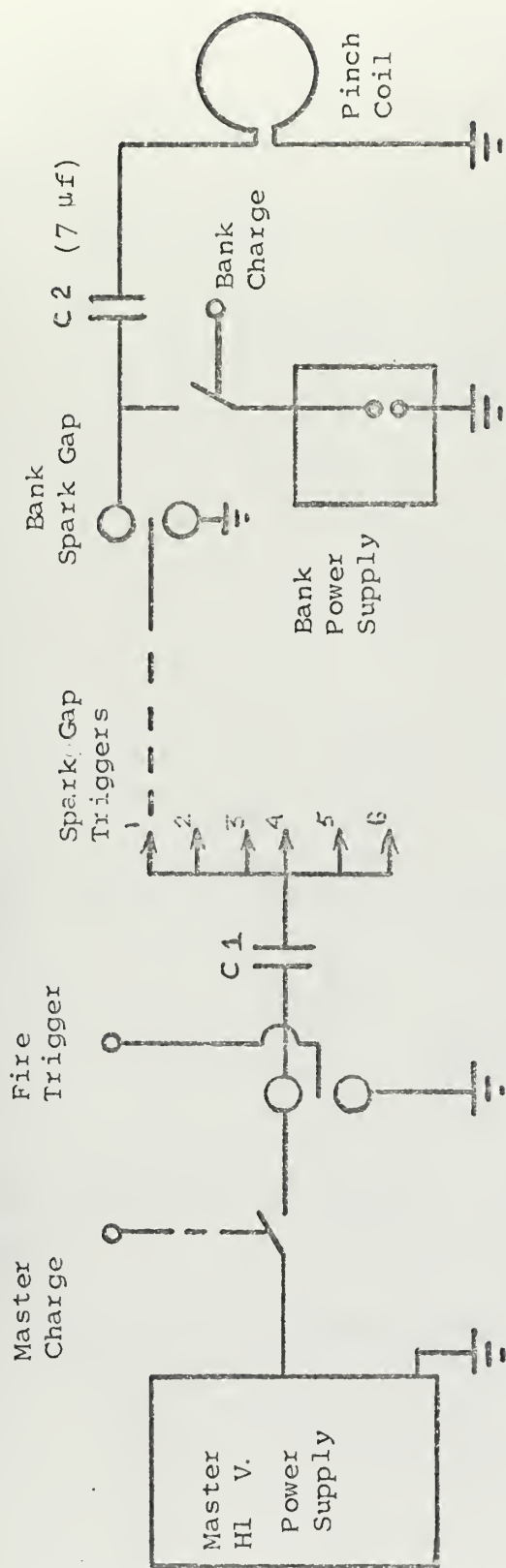
BASIC OPERATION

Master H.V.P.S. provides up to 50 kV across Master Gap charging C 1.
Depressing Fire button initiates a 50 kV trigger pulse across Master Gap,
discharging C 1 and thus providing 6 separate triggers to the Main Bank
Spark Gaps. These break down discharging C 2 (one of 6 7μf cap.) through
pinch coil. .

Figure 3A. System Block Diagram

MASTER SPARK GAP CIRCUIT
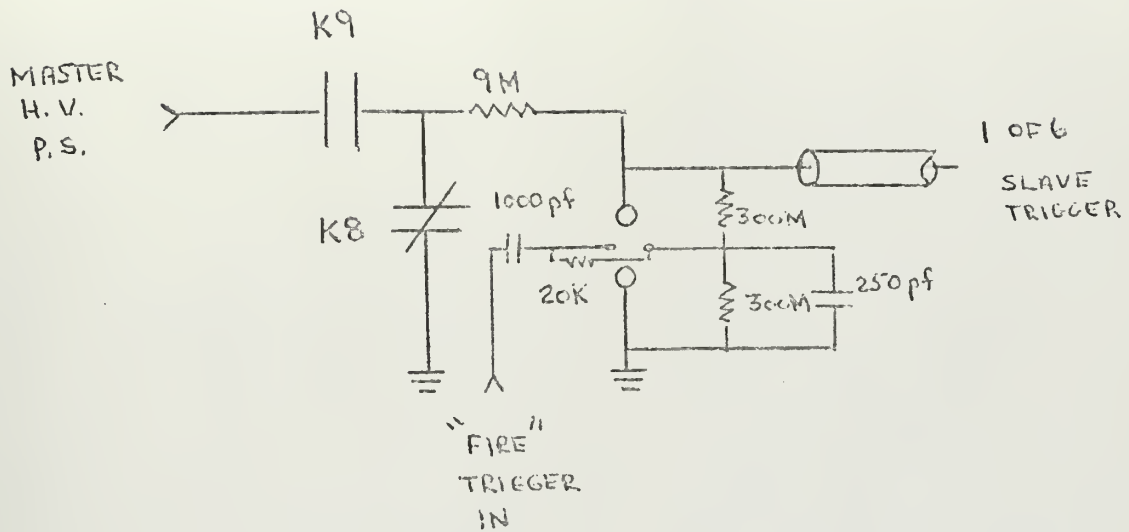
MAIN BANK SPARK GAP CIRCUIT
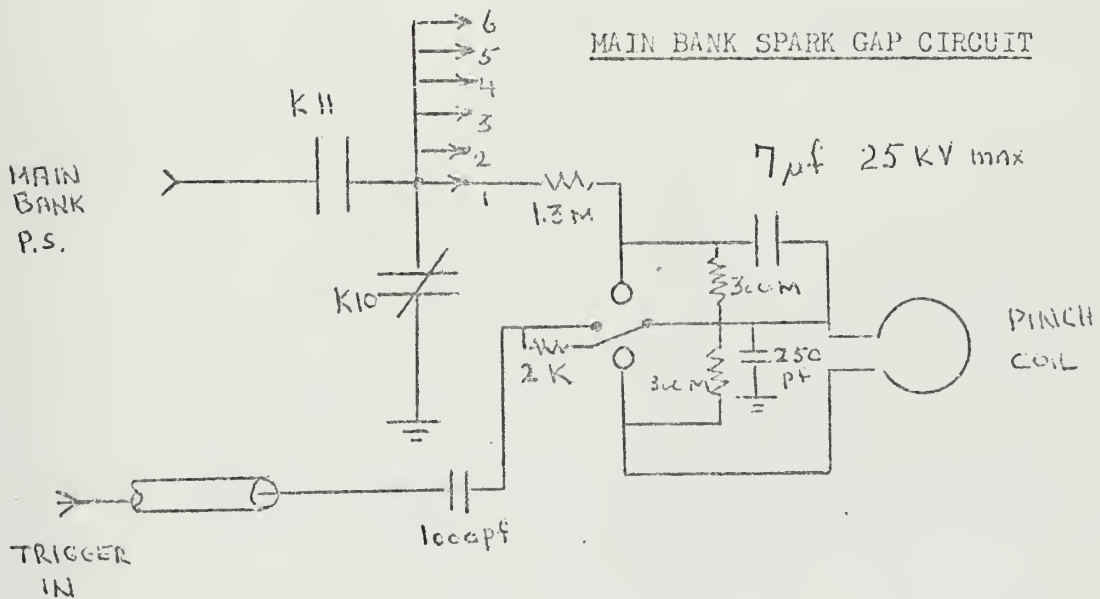
K8,K9,K10,K11 SEQUENCED VACUUM RELAYS

Figure 3B.   System Schematic
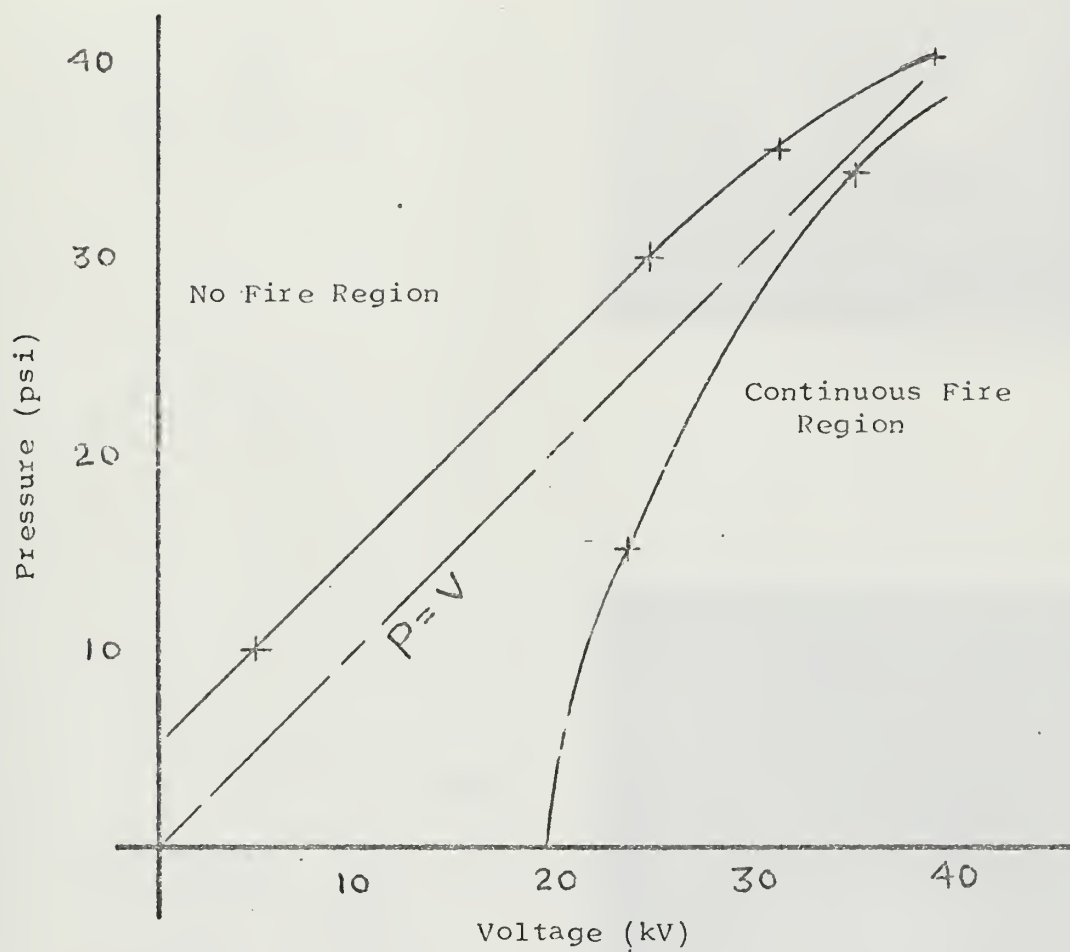
Figure 4. Pressure Voltage Characteristics

Trace starts at
second gridline to
right.

5a. Air
Horizontal scale 1 µsec/div
Vertical scale   1 V/div
Frequency ~ 110 kHz
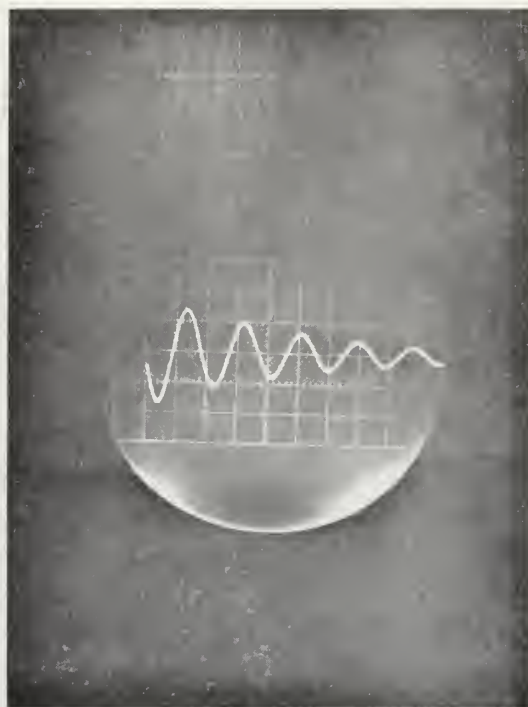
5b. Neutral Argon

Upper trace
  H. scale 10 µsec/div
  V. scale 1 V/div
  Frequency ~ 110 kHz

Lower trace
  H. scale 50 µsec/div
  V. scale .5 mv/div
  Frequency ~ 20 kHz
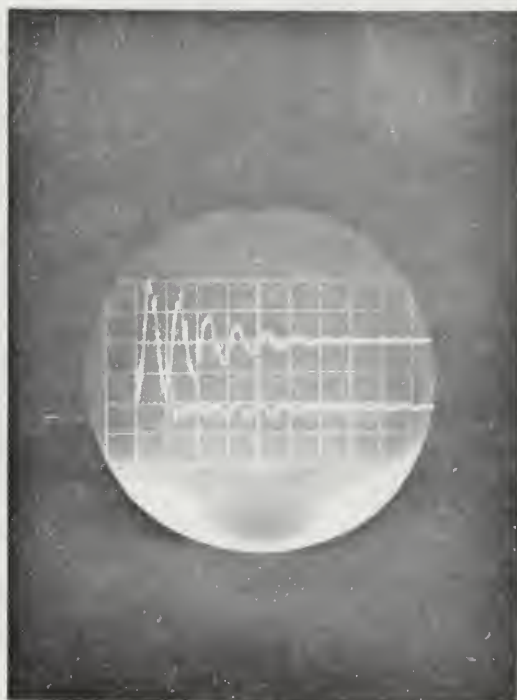
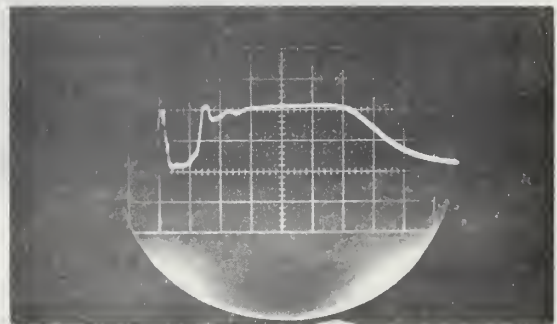Figure 5.   Theta Pinch Coil Ringing Frequency
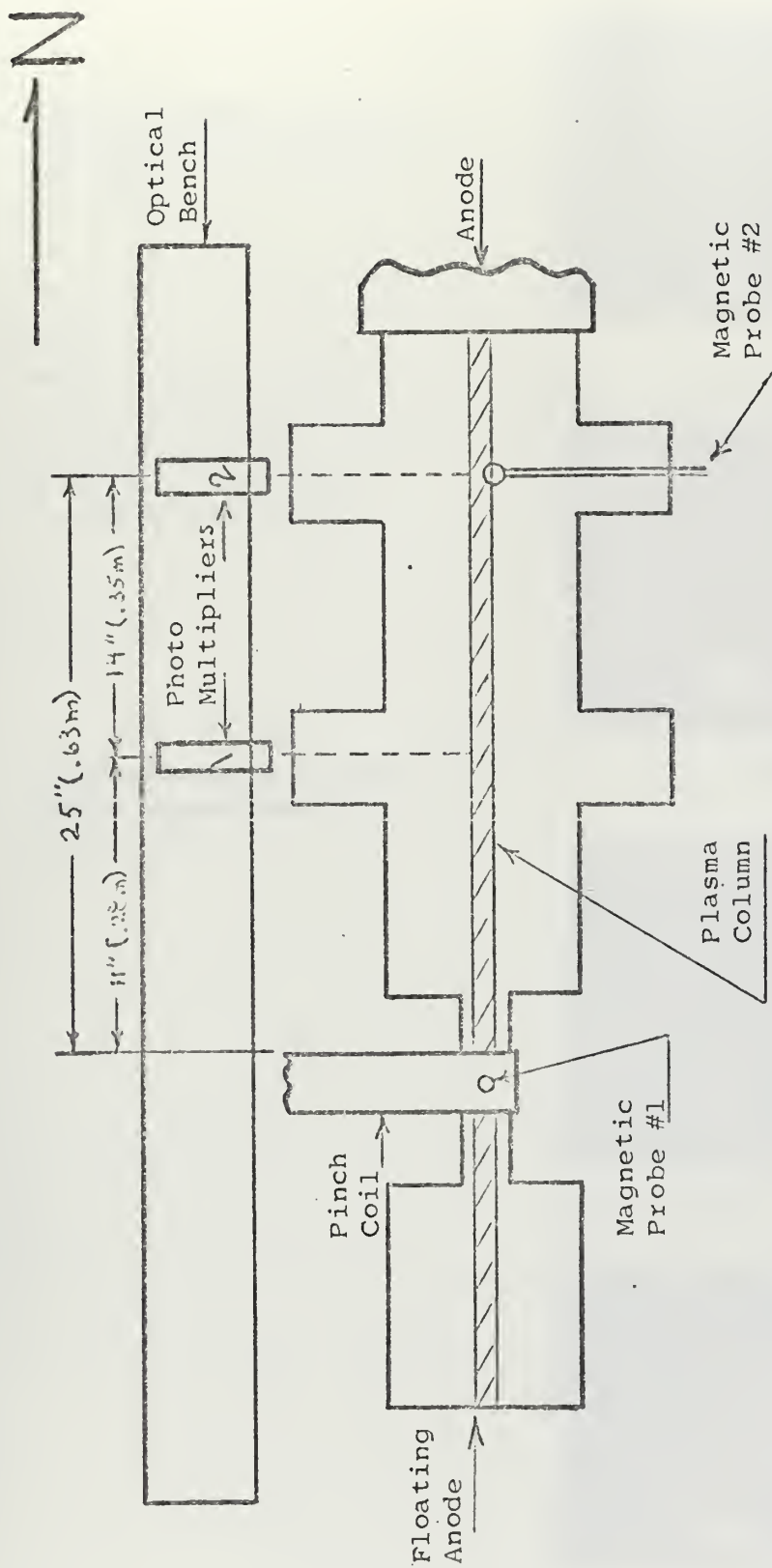
Figure 6. Experiment Configuration

53

Neutral Argon traces
start at second gridline
to right

Bank Voltage 15 kV

Column Pressure 0.1 Torr
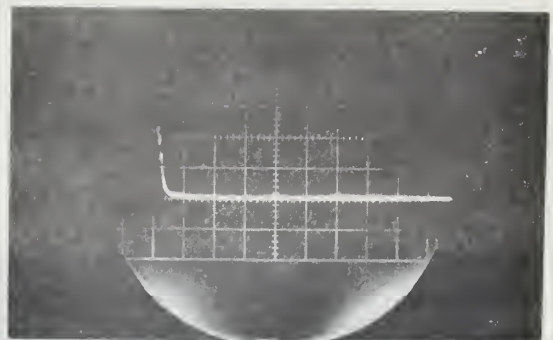
H. scale 100 μsec/div

V. scale 100 mV/div

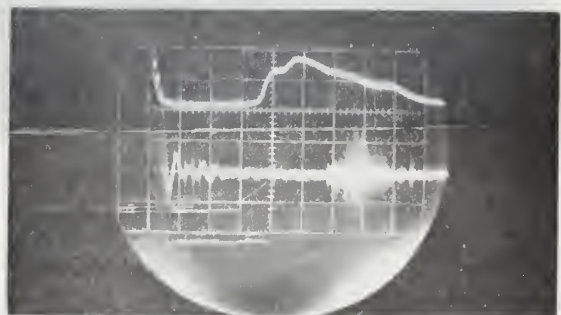Photomultiplier located
.635 m downstream from
pinch coil

a. B_o = 900G

b. B_o = 1800G

c. B_o = 0
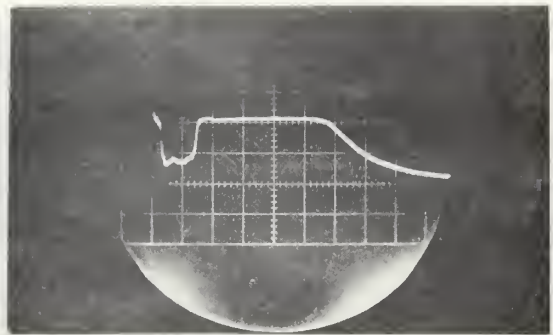
d. B_o = 1800G
    4 capacitors discharged

Figure 7. Hydrodynamic Shock Front Profiles
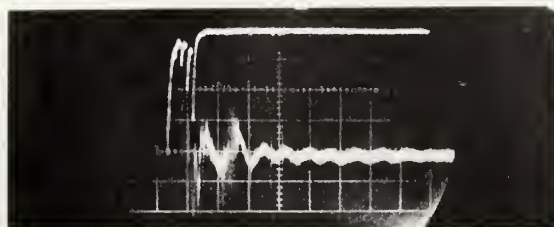
54

Argon Plasma

Column Pressure 10^{-4} Torr

B_o = 1800G
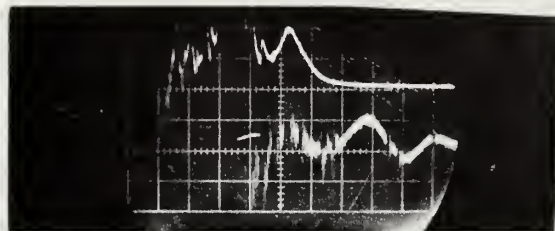
Photomultiplier located at
.625 m

50 μsec/div

Upper trace
Photomultiplier output
100 mV/div
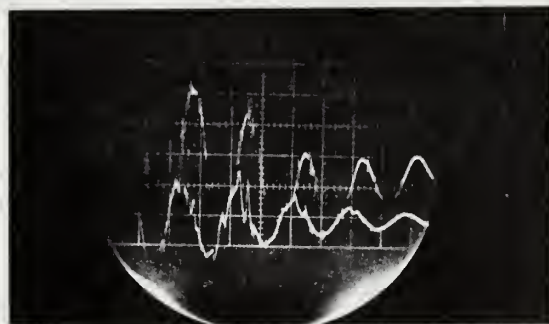
Lower trace
Magnetic probe output
0.5 mV/div

20 μsec/div

Figure 8.   Plasma Shock Front Generation

Neutral Argon Gas
B_o = 3600G
Upper Trace
Magnetic probe at .635 m
downstream from pinch coil

Lower trace
Theta Pinch magnetic probe

5 μsec/div

Phase separation ~ 2 μsec

$\overline{V}$ ~ 300 km/sec

Figure 9.   "Kink" Propagation Characteristics

55

REFERENCES

1. R.C. Andrews, Shock Production, Langmiur Probe Diagnostics, and Instabilities in a Nitrogen Plasma, Naval Postgraduate School Thesis (1968).

2. J.C. Beam, Investigations in the Vacuum Ultraviolet of a Steady State Nitrogen Plasma, Naval Postgraduate School Thesis (1969).

3. D.M. Budzik, Construction of a Theta-Pinch for the Generation of Shock Waves in a Nitrogen Plasma, Naval Postgraduate School Thesis (1970).

4. R.Z. Sagdeev, Cooperative Phenomena in Collisionless Plasmas, Review of Plasma Physics, 4, Consultants Bureau, (1966).

5. T.J.M. Boyd and J.J. Sanderson, Plasma Dynamics, Barnes and Noble, Inc., New York, (1969).

6. D.J. Rose and M. Clark Jr., Plasmas and Controlled Fusion The Massachusetts Institute of Technology Press and John Wiley and Sons, Inc., (1961).

7. H.W. Liepman and A. Roshko, Elements of Gasdynamics, John Wiley and Sons Inc., (1957).

8. Ya. B. Zel'dovich and Yu. P. Raizer, Physics of Shock Waves and High-Temperature Hydrodynamic Phenomena, Vols. I, II, Academic Press (1966, 1967).

9. V.D. Shafranov, The Structure of Shock Waves in a Plasma, Soviet Physics, JETP, 5, 1183-1188 (1957).

10. Jukes, J.D., The Structure of a Shock Wave in a Fully Ionized Gas, J. Fluid Mech. 3, 275-285 (1957).

11. M.Y. Jaffrin and R.F. Probstein, Structure of a Plasma Shock Wave, Phys. of Fluids, 7, 1658-1674, (1964).

12. T.A. McLaughlin, Inductive Magnetic Probe Diagnostics in a Plasma, Naval Postgraduate School Thesis (1970).

INITIAL DISTRIBUTION LIST

		No. Copies
1.	Defense Documentation Center Cameron Station Alexandria, Virginia 22314	2
2.	Library, Code 0212 Naval Postgraduate School Monterey, California 93940	2
3.	Assoc. Prof. A.W.Cooper, Code 61 Cr Department of Physics Naval Postgraduate School Monterey, California 93940	4
4.	LT Charles L. Christensen 1011 Warren Street Utica, New York 13503	1

DOCUMENT CONTROL DATA - R & D

(Security classification of title, body of abstract and indexing annotation must be entered when the overall report is classified)

1. ORIGINATING ACTIVITY (Corporate author)	2a. REPORT SECURITY CLASSIFICATION
Naval Postgraduate School Monterey, California 93940	Unclassified
	2b. GROUP

3. REPORT TITLE

Investigation of Theta-pinch Produced Shock Waves in a Plasma

4. DESCRIPTIVE NOTES (Type of report and, inclusive dates)

Master's Thesis: June 1971

5. AUTHOR(S) (First name, middle initial, last name)

Charles L. Christensen

6. REPORT DATE	7a. TOTAL NO. OF PAGES	7b. NO. OF REFS
June 1971	59	12

8a. CONTRACT OR GRANT NO.	9a. ORIGINATOR'S REPORT NUMBER(S)
b. PROJECT NO.	
c.	9b. OTHER REPORT NO(S) (Any other numbers that may be assigned this report)
d.	

10. DISTRIBUTION STATEMENT

Approved for public release; distribution unlimited.

11. SUPPLEMENTARY NOTES	12. SPONSORING MILITARY ACTIVITY
	Naval Postgraduate School Monterey, California 93940

13. ABSTRACT

This report discusses the completion and operational testing of the theta pinch experiment at the Naval Postgraduate School Plasma Facility. The system consists of a 42 μF capacitor bank feeding a single turn theta pinch coil with a total energy capacity of 13.1 kJ. Included is a brief discussion of the theory of shock wave generation and propagation in a plasma along with experimental verification of reproducible hydro-dynamic shock waves of Mach ~ 16 produced in a neutral Argon gas at 0.1 torr. Calculations based on the theory of shock wave thicknesses (3 cm.) are compared to observed values (10 cm.) at this pressure. An outline of proposed future experiments at the Plasma Facility is included in the recommendations.

DD FORM 1473 (PAGE 1)
1 NOV 65

S/N 0101-807-6811

KEY WORDS	LINK A		LINK B		LINK C	
	ROLE	WT	ROLE	WT	ROLE	WT
Theta Pinch						
Collisionless Plasma						
Collisionless Shock Front						
Viscous Shock Front						
Electron heat conduction						